

Rapid estimates of leaf litter chemistry using reflectance spectroscopy

Shan Kothari 📭 , Sarah E. Hobbie , and Jeannine Cavender-Bares a,b

^aDepartment of Plant and Microbial Biology, University of Minnesota, 1479 Gortner Ave, St. Paul, MN 55108, US; ^bDepartment of Ecology, Evolution, and Behavior, University of Minnesota, 1479 Gortner Ave, St. Paul, MN 55108, US

Corresponding author: Shan Kothari (email: shan.kothari@umontreal.ca)

Abstract

Measuring the chemical traits of leaf litter is important for understanding plants' influence on nutrient cycles, including through nutrient resorption and litter decomposition, but conventional leaf trait measurements are often destructive and labor-intensive. Here, we develop and evaluate the performance of partial least-squares regression models that use reflectance spectra of intact or ground leaves to estimate leaf litter traits, including carbon and nitrogen concentration, carbon fractions, and leaf mass per area (LMA). Our analyses included more than 300 samples of senesced foliage from 11 species of temperate trees, including both needleleaf and broadleaf species. Across all samples, we could predict each trait with moderate-to-high accuracy from both intact-leaf litter spectra (validation $R^2 = 0.543-0.941$; %root mean squared error (RMSE) = 7.49–18.5) and ground-leaf litter spectra (validation $R^2 = 0.491-0.946$; %RMSE = 7.00–19.5). Notably, intact-leaf spectra yielded better predictions of LMA. Our results support the feasibility of building models to estimate multiple chemical traits from leaf litter of a range of species. In particular, intact-leaf spectral models allow non-destructive trait estimation in a matter of seconds, which could enable researchers to measure the same leaves over time in studies of nutrient resorption.

Key words: decomposition, functional traits, nutrient cycling, nutrient resorption, reflectance spectroscopy

Introduction

Long-lived plants resorb and store a large fraction of the nutrients from their leaves before they senesce. These reserves support early growth in the following growing season and reduce the need for nutrient uptake from the soil (El Zein et al. 2011). However, nutrient resorption (much like soil nutrient uptake) has metabolic and physiological costs, so the optimal level of nutrient resorption varies among environments (Wright and Westoby 2003). Accordingly, plants vary broadly in their nutrient resorption efficiency—the fraction of a given nutrient that is resorbed (Vergutz et al. 2012). For example, plants often (Kobe et al. 2005; Hayes et al. 2014; Yuan and Chen 2015), though not always (Diehl et al. 2003), resorb a greater fraction of leaf nutrients when soil nutrients are scarce. This adjustment of resorption efficiency in response to the environment highlights the key role of resorption in plant nutrient economics.

Resorption often leaves the resulting leaf litter relatively nutrient-poor, which can limit the rate of decomposition of newly shed litter by soil microorganisms (Berg 2014). Hence, nutrient-poor litter decomposes more slowly than nutrient-rich litter at first (Cornwell et al. 2008), although this trend can reverse in later stages (Prescott 2010; Berg 2014; Gill et al. 2021). Because litter nutrient levels influence the nutrient flux into soil inorganic or microbial pools via decomposition, resorption may be an important process for explaining how

plants influence their environment (Hobbie 2015). Although many metabolic changes occur during senescence, fresh-leaf and leaf litter composition often remain correlated, which may help explain why soil processes can often be inferred from remote sensing of aboveground vegetation (Madritch et al. 2020; Cavender-Bares et al. 2022).

Addressing many ecological questions about nutrient resorption and litter decomposition requires measuring litter chemistry. Because estimating resorption efficiency requires knowing the nutrient content of leaves both before and after senescence, it can be expensive and labor-intensive. Furthermore, because measuring nutrient concentration through elemental analysis is destructive, the same exact leaves cannot be measured at each step. Decomposition also depends on litter traits beyond macronutrient concentrations, including lignin, cellulose, condensed tannins, and various micronutrients (Schweitzer et al. 2004; Cornwell et al. 2008; Talbot and Treseder 2012; Keiluweit et al. 2015; Bourget et al. 2023). The potential number of traits and samples can add up to make research on leaf litter and nutrient cycling expensive and time consuming.

The cost and time involved may make it harder to understand and predict the fluxes of carbon and mineral nutrients between plants, litter, and soil—the determinants of which are still far from well-understood. For example, large-scale comparative tests of the role of nutrient resorption in plant

life history or nutrient economics are still rare (e.g., Freschet et al. 2010; Rea et al. 2018). Meanwhile, research continues to reveal new paths through which a plant community's litter traits or diversity interact with microbial communities and the abiotic environment to influence decomposition rates (Grossman et al. 2020; Liu et al. 2020; Gill et al. 2021; Bourget et al. 2023). Fast, simple estimates of litter traits could make it easier both to study the functional significance of nutrient resorption and to estimate litter decomposability rapidly across taxa and ecosystems.

The need for faster trait estimates has led some plant ecologists to turn to reflectance spectroscopy, a technique that involves measuring the reflectance of radiation from a sample across many wavelengths. Many kinds of samples, including leaf tissue, are analyzed using the 400–2400 nm range. Reflectance in this range can be used to estimate many leaf structural and chemical traits because those traits influence how leaves scatter and absorb radiation across wavelengths.

Many widely studied functional traits nevertheless cannot be identified with unique, distinct absorption features. For example, the leaf dry matter that contributes to leaf mass per area (LMA) includes varying fractions of macromolecules like non-structural carbohydrates, hemicellulose, cellulose, lignin, and proteins, which have varying, broad, and overlapping optical features (Curran 1989). This challenge is among the reasons that many plant scientists have adopted a multivariate empirical approach to linking traits and reflectance spectra using statistical techniques like partial least-squares regression (PLSR; Wold 1994; Burnett et al. 2021). The hope is that these approaches can flexibly "learn" relationships from actual data rather than assuming that complex traits have fixed and pre-specified relationships with optical features (Curran 1989). Researchers have built PLSR models predicting traits like LMA and nitrogen concentration with a high degree of accuracy from reflectance spectra, measured either while the leaf was fresh or after drying and grinding it into powder (Serbin et al. 2014, 2019; Kothari et al. 2023a, 2023b). Further research has shown that spectral models can predict traits as varied as defense compounds (Couture et al. 2016), water status (Asner et al. 2011; Cotrozzi et al. 2017; Kothari et al. 2023a), leaf age (Chavana-Bryant et al. 2017), and photosynthetic capacity (Dechant et al. 2017).

The vast majority of this research is based only on measurements taken during the growing season, before the onset of leaf senescence. These models are not expected to accurately predict the traits of senesced leaves, which have undergone metabolic and physical changes that alter their chemical composition and spectra, bringing them well outside typical ranges observed in fresh green leaves (Gillon et al. 1999a). Some researchers have built models to predict decomposition-related traits (Joffre et al. 1992; McTiernan et al. 2003; Coûteaux et al. 2005; Hobbie 2005; Parsons et al. 2011; Petit Bon et al. 2020) or the decomposition rate itself (Gillon et al. 1999b; Fortunel et al. 2009; Parsons et al. 2011) from ground-leaf litter using near-infrared (NIR) reflectance spectroscopy. Many traits that influence decomposition also influence forage quality, and there is an extensive body of research predicting forage traits using NIR spectroscopy, including in senescent foliage (e.g., Norris et al. 1976). Such studies have often shown high accuracy ($R^2 > 0.9$) in predicting traits like N_{mass} , carbon fractions, and phenolics, although these models have usually been calibrated using a limited number (<120) of samples from one or a few species.

Here, we expand on prior work by building models to predict traits related to litter quality and recalcitrance from reflectance spectra. Compared to previous studies, we calibrate and validate our models using more samples from more species. This breadth allows us to make predictions over a wide range of trait values and test how well models predict both intra- and interspecific trait variation. We also measured spectra from the same samples both while intact and ground. Existing models to predict leaf litter traits require the destructive and time-consuming step of grinding the tissue, which motivated us to test whether spectra of whole, intact litter could also yield accurate estimates. We predicted that ground-leaf litter spectra would provide more accurate estimates of chemical traits than intact-leaf litter spectra, as most comparisons on non-senesced leaves have shown (Serbin et al. 2014; Couture et al. 2016; Kothari et al. 2023b). On the other hand, we predicted that intact-leaf litter spectra would outperform ground-leaf litter spectra for estimating structural traits like LMA because grinding destroys the leaf structure (Kothari et al. 2023b).

Finally, we verified whether our litter chemistry estimates could capture known differences among functional groups. We predicted that conifer litter would have greater LMA, recalcitrant carbon, and C_{mass} and lower N_{mass} than broadleaf litter. These patterns are thought to explain much of why conifer litter tends to show slower initial decomposition rates than broadleaf litter (Cornelissen et al. 1999; Cornwell et al. 2008; Prescott 2010).

Methods

Samples

During fall 2018, we collected senescent leaf litter from the Forests and Biodiversity (FAB1) experiment at Cedar Creek Ecosystem Science Reserve (East Bethel, MN, USA; Grossman et al. 2017). In May 2013, one- to two-year-old trees were planted in a $0.5~{\rm m}\times0.5~{\rm m}$ grid within plots that varied in their species richness (1, 2, 5, or 12 species) and composition. The species pool included eight broadleaf angiosperms and four needleleaf conifers (Table 1). We left out one species (Juniperus virginiana) from sampling because its scaly needle morphology meant that individual trees seldom produced enough litter at once for spectroscopic or chemical analyses. To get enough samples of another species (Acer negundo), we also collected material from mature trees in a residential yard in Minneapolis, MN, USA, $50.0~{\rm km}$ from FAB1.

We collected litter samples as close as we feasibly could to the time of senescence using both litterfall traps on the ground and hand-collection of senesced leaves from trees. We only took leaves from trees when the petiole had a complete abscission layer and the leaf could be detached with a gentle pull (Chapin and Moilanen 1991). Because species dropped their leaves at different times, we collected litter repeatedly from September to November 2018 to ensure that the litter

Table 1. Details of species in the Forests and Biodiversity (FAB1) experiment.

Species	Code	Functional group	No. of samples
Acer negundo L.	ACNE	Broadleaf	27
Acer rubrum L.	ACRU	Broadleaf	28
Betula papyrifera Marshall	BEPA	Broadleaf	36
Juniperus virginiana L.	JUVI	Needleleaf	n/a
Pinus banksiana Lamb.	PIBA	Needleleaf	20
Pinus resinosa Aiton	PIRE	Needleleaf	31
Pinus strobus L.	PIST	Needleleaf	26
Quercus alba L.	QUAL	Broadleaf	37
Quercus ellipsoidalis E.J. Hill	QUEL	Broadleaf	33
Quercus macrocarpa Michx.	QUMA	Broadleaf	34
Quercus rubra L.	QURU	Broadleaf	33
Tilia americana L.	TIAM	Broadleaf	17
Total			322

Note: All broadleaf species listed are deciduous angiosperms, and all needleleaf species are evergreen conifers. We did not sample *Juniperus virginiana*. Twelve of the *Acer negundo* samples come from a residential yard rather than FAB1. One *Betula papyrifera* sample included in the tally was omitted from ground litter analyses due to lack of tissue.

we collected had recently senesced. To avoid influence from leaching we discarded litter samples from traps after rain, although nitrogen and carbon leaching tends to be low even under extreme wetting (Schreeg et al. 2013).

We collected 322 litter samples, seeking to represent the variation in leaf traits within each species (n = 17-37 per species; Table 1). While our sampling did not explicitly account for the species richness and composition treatments in FAB1, we collected leaves from each species across neighborhoods and crown positions to enhance intraspecific variation. In some cases, we selected multiple leaves from distinct crown positions on the same tree. Each sample included 1.5-3.0 g of tissue and could comprise one leaf or multiple similar leaves. When a single trap contained more than 2.5-3.0 g of leaves from a single species, we divided them into two or more samples by keeping together leaves that we judged by eye to be more visually similar. We dried each sample in a dark shed at 40 °C for at least 3 days, and then stored them in a cool, dark room until spectral and trait measurements.

Spectral data collection

We measured reflectance spectra of each dried sample using a PSR+ 3500 full-range (350–2500 nm) spectrometer (Spectral Evolution, Lawrence, MA, USA). Each sample's spectrum was measured both in its intact state and after grinding. For intact-leaf spectra, we used the Spectral Evolution leaf clip assembly. This leaf clip covers a surface area of around 1 cm² and has an angle of incidence of 30° from surface normal. We used a built-in 99% Spectralon white reflectance standard to calibrate readings before each sample. Among broadleaf species, we always measured the adaxial side; many leaves curled in on themselves during senescence and drying, but we sought to measure spectra in relatively flat portions of the leaf to minimize specular reflection (Petibon et al. 2021). Among needleleaf species, we made mats by laying out

needles in a single layer; although we aimed to reduce gaps or areas of overlap between needles, there usually remained some due to their shape. On each sample, we measured multiple spectra from distinct places. We discarded spectral measurements with large discrepancies in sensor overlap regions, or (particularly for needleleaf species) with very high (>70%) or very low (<30%) maximum reflectance, which often indicated that the needle mat was highly non-uniform. There remained at least three reflectance spectra for nearly all samples. (For five conifer samples, we retained only two replicate spectra due to challenges in obtaining good measurements.) For some broadleaf samples comprising many small leaves, we measured more than 10 spectra to capture a representative sample.

After removing their petioles, we ground leaf samples by placing them in individual plastic vials with ball bearings and shaking them with a paint shaker for several hours, pulverizing them into a fine powder. To measure ground-leaf spectra, we used the Spectral Evolution benchtop reflectance probe and glass-windowed sample trays. Before measuring each sample, we measured a white Spectralon panel placed in a sample tray for calibration. For sample measurements, we put at least 0.6 g of leaf powder into a sample tray. Preliminary tests showed that adding more material did not change the spectra, suggesting that transmittance was close to zero. The benchtop probe pressed the loose powder into an even pellet. We measured three spectra per sample—turning the sample tray 120° between the first two measurements, and loosening and mixing the powder between the second and third measurements.

The spectrometer automatically interpolated the spectra to 1 nm resolution. We performed all subsequent processing using *spectrolab v. 0.0.18* (Meireles et al. 2023) in *R v. 4.2.1* (R Core Team 2022). Because the 2400–2500 nm and especially the 350–400 nm region could be noisy (Petibon et al. 2021), we trimmed each spectrum to 400–2400 nm. For intact leaves only, we corrected discontinuities at the overlap region be-

tween the Si and first InGaAs detectors (970–1000 nm) using the *match_sensors* function, and spline-smoothed only this region using the *smooth_spline* function. Finally, we averaged all intact spectra and all ground spectra for a given sample. As a metric of measurement consistency, we calculated the mean spectral angle between measurements of the same sample (Kruse et al. 1993). Intact measurements (median across samples: 6.8°; 2.5th–97.5th percentile: 2.9°–20.4°) showed much less consistency than ground measurements (median: 0.6°; 2.5th–97.5th percentile: 0.2°–3.2°).

Trait measurements

We measured a relatively simple set of leaf litter traits that are useful for understanding plants' influence on nutrient cycles: soluble contents, hemicellulose, recalcitrant carbon (largely cellulose and lignin), total carbon and nitrogen concentrations, and LMA. Most of these traits have a demonstrated role in explaining decomposition rates across sites (Cornwell et al. 2008), although we acknowledge that decomposition is a complex, dynamic process that can be influenced by many other traits. Both nitrogen concentration and LMA are also essential for quantifying nitrogen resorption.

Leaf mass per area

Researchers risk underestimating resorption efficiency when they fail to account for leaf mass loss during resorption. To avoid this risk, many studies either express nutrient content of non-senesced and senesced leaves on a per-area basis, or equivalently include a mass loss correction factor (van Heerwaarden et al. 2003). We measured LMA of each litter sample to enable conversion between a per-mass and per-area basis. We did not attempt to quantify or correct for the smaller bias sometimes caused by leaf shrinkage (van Heerwaarden et al. 2003).

For broadleaf species, we could not measure the area of whole leaves because many were curled and brittle. Instead, we used a hole punch to take four to six 0.3 cm² disks from each dried leaf sample. We sought to capture the variation within the sample, including veins. We calculated LMA as the total mass divided by the total area of all disks. This method has generally been shown to provide accurate estimates of the LMA of whole leaves (Perez et al. 2020).

For needleleaf species, we measured the mass and area of five needles per sample. We estimated area as the length times the maximum width of the needle measured using digital calipers. We then measured the mass of each needle and calculated LMA as the total mass divided by the total area.

Chemical traits

We measured leaf carbon and nitrogen concentration (C_{mass} and N_{mass}) on ground, oven-dried samples using dry combustion gas chromatography performed by an elemental analyzer (Costech ECS 4010 Analyzer, Valencia, California, USA). We converted C_{mass} and N_{mass} to an area basis (C_{area} and N_{area}) by multiplying them with LMA. We only trained mod-

els for these area-based traits from intact-leaf spectra. We had noticed that models for LMA trained on ground-leaf spectra showed poorer performance than those trained on intact-leaf spectra, especially at capturing intraspecific variation ("Results" section); as a result, we decided that it would be imprudent to estimate other traits defined on an area-basis from intact-leaf spectra.

We measured carbon fractions on ground, oven-dried samples using an ANKOM 200 Fiber Analyzer to carry out a sequential digestion protocol (Ankom Technology, Macedon, New York, USA). The first digestion in a hot neutral detergent solution washes out plant solubles. The second digestion in a hot acidic detergent solution further washes out bound proteins and hemicellulose (henceforth "hemicellulose" for simplicity). The remaining fraction comprises cellulose and acid-unhydrolyzable residue (AUR) such as lignin (henceforth "recalcitrant carbon"). We estimated each component using the changes in sample mass between steps. Because the paint shaker ground our samples into a very fine powder, we had to use small-pored ANKOM F58 fiber bags, which cannot be used in the final acid detergent lignin digestion to measure AUR concentration alone. We also did not determine the ash concentration of the samples.

We removed some trait values prior to statistical analyses because of clear issues during trait data collection—for example, the rupture of sample bags while measuring carbon fractions. Unlike some other studies (e.g., Gillon et al. 1999b), we only removed samples due to known issues with trait measurements, not simply because they had large prediction residuals during statistical analyses.

Partial least-squares regression analyses

We modeled the relationship between traits and spectra using PLSR, which is well suited to handle datasets that include many collinear predictors (Wold 1994; Burnett et al. 2021). PLSR reduces the full samples \times wavelengths matrix to a smaller number of orthogonal latent components that best explain the variation in the variables to be predicted. We implemented our PLSR models in R package $pls\ v.\ 2.8.3$ (Mevik et al. 2019).

Previous studies using a PLSR modeling framework have often restricted the range of wavelengths used to predict certain traits to select bands that, based on prior research or known absorption features, may be most causally linked to the traits in question (e.g., Serbin et al. 2014). In our main set of analyses, we used the full spectrum (400–2400 nm) to predict each trait on the grounds that biochemical changes during senescence may alter the relationship between integrative functional traits like N_{mass} and specific optical features. However, we also explored two ways of restricting the spectral range for intact-leaf spectra only. First, we built models using only 400-1000 nm ("visible/near infrared range (VIS/NIR) models") given that many less-expensive spectrometers only measure this range. Second, we built models using only 1300-2400 nm ("short-wave infrared range (SWIR) models") since the pigment composition of leaves changes rapidly during senescence, including breakdown products ("brown pigments") that may absorb up to 1300 nm (Fourty et al. **1996**). The SWIR models could perform better in cases where pigments are poor indicators of the overall composition of the leaf.

Researchers may transform reflectance of ground-leaf spectra to pseudoabsorbance ($-\log R$) or its derivatives (Blackburn 1998; Reeves 2009), which may somewhat linearize the relationship between traits and spectral features and make those features more prominent. We found in preliminary tests that these transformations did not substantially improve model performance. Likewise, brightness normalization of intactleaf spectra (Feilhauer et al. 2010) did not have a strong influence on model performance.

We divided our samples into calibration (75%) and validation (25%) datasets, stratified such that the proportions of each species were identical in each dataset. We fit models for each trait on the complete calibration dataset, using 10-fold cross-validation to select the optimal number of model components to use in further analyses while avoiding overfitting. We selected the smallest number of components whose cross-validation root mean squared error of prediction (RM-SEP) was within one standard deviation of the very lowest RMSEP at any number of components. We used these models to calculate the variable importance in projection metric (VIP) for each trait (Wold 1994) but we do not report their accuracy.

We developed our main set of models using a resampling procedure in which we divided the calibration data at random 200 times into 70% training and 30% testing subsets (Burnett et al. 2021). During each resampling iteration, we trained a model for each trait on the 70% and assessed its performance (RMSE and R^2) on the remaining 30%, using the previously determined number of components for that trait. This procedure left us with an ensemble of 200 models for each trait, which could be used both to make trait predictions and to examine the variability of model performance under random variation in training data.

We used these ensembles of models to predict traits from the validation (25%) dataset. We quantified model performance for each trait by calculating R² and root mean squared error (RMSE) between the predictions (averaged for each validation sample across the 200 estimates) and the measured values. We also report the %RMSE, calculated as the RMSE divided by the 2.5% trimmed range of the measured values in the validation data (Kothari et al. 2023a). This metric allows the amount of error in trait estimates to be assessed relative to the actual range of variation.

Spectral indices of pigment contents

Since our analyses of spectral variation and VIP ("Results" section) suggested that wavelengths sensitive to pigment contents were important for predicting several traits in both full-range and VIS/NIR models, we calculated two spectral indices used to assess pigment status in senescing leaves. The first is the plant senescence reflectance index (PSRI) of Merzlyak et al. (1999), calculated as PSRI = $(R_{678} - R_{500})/R_{750}$, where R_n is the reflectance at n nm. This index correlates positively with carotenoid : chlorophyll ratios, which increase during leaf senescence because chlorophyll degrades sooner than

carotenoids. The other index is the red-edge chlorophyll index (CI_{RE}) of Gitelson et al. (2009), calculated as CI_{RE} = ρ_{NIR}/ρ_{RE} – 1, where ρ_{NIR} is the mean reflectance across 760–800 nm (part of the NIR range) and $\rho_{\rm RE}$ is the mean reflectance across 690-710 nm (part of the red edge). This index is closely linked to chlorophyll content. We used Analyses of covariance (AN-COVA) with Type III sums of squares to test whether these indices, species identity, and their interaction are related to traits, with the aim of evaluating the main effect of the indices. We ran analyses separately for the two indices and for intact- and ground-leaf spectra, and focused on two traits (N_{mass} and recalcitrant carbon) for the purpose of demonstration. In particular, leaf nitrogen and chlorophyll are often tightly correlated in fresh leaves, although the strength and slope of this correlation varies by species and growing conditions (Dechant et al. 2017).

Results

There was a high level of variation in each trait both across the entire dataset and within species. At one extreme, N_{mass} varied nearly 11-fold across the entire dataset; at the other, C_{mass} only varied about 1.5-fold (Table 2). In spite of the high intraspecific variation in some traits, linear regressions of traits against species identity showed that between 46.0% (R² for N_{area}) and 93.7% (R² for LMA) of trait variation could be explained by species identity alone. In general, needleleaf species had much higher LMA, C_{mass}, recalcitrant carbon, and lower N_{mass} than broadleaf species (Table S1), consistent with trends in non-senescent leaves (Serbin et al. 2014; Kothari et al. 2023a). Consequently, we see correlations among pairs of litter economic traits (sensu Freschet et al. 2012) across the whole dataset (for log(LMA) and $log(N_{mass})$, $R^2 = 0.592$; $p < 10^{-15}$), but a weaker correlation among just needleleaf samples ($R^2 = 0.255$; $p < 10^{-5}$) and none among just broadleaf samples ($R^2 = 0.011$; p = 0.111).

Among both ground-leaf and intact-leaf spectra, the coefficient of variation (CV) was highest in the visible range and decreased into the NIR range (Fig. 1). For intact-leaf spectra only, the CV once again increased into the SWIR. There was a global maximum CV around 440–490 nm for intact spectra, shifted to lower wavelengths for ground spectra; there were also local maxima centered at around 670–675 nm for both kinds of spectra.

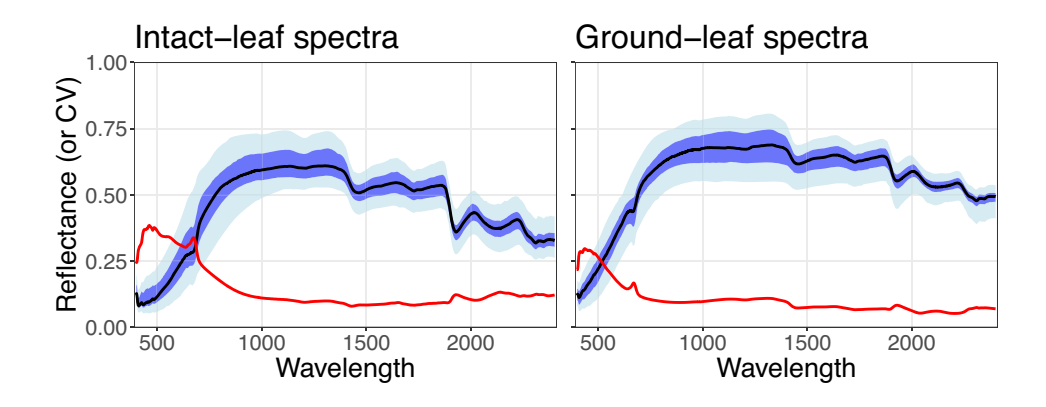
Each of our traits could be predicted with moderate-to-high success from full intact-leaf and ground-leaf spectra (Figs. 2–4; Table 2). The models for N_{mass} and (especially for intact-leaf spectra) LMA achieved the highest validation accuracy, followed by recalcitrant carbon, solubles, C_{mass} , and finally hemicellulose (Table 2). There was no general tendency for estimation of chemical traits to be better using intact- or ground-leaf spectra, but estimation of LMA was better using intact-leaf spectra. We built models predicting N_{area} and C_{area} only from intact-leaf spectra (Fig. 4). The C_{area} model (%RMSE = 8.02) had better performance than the C_{mass} model (%RMSE = 14.0), but the N_{area} model (%RMSE = 13.2) had worse performance than the N_{mass} model (%RMSE = 8.58; Table 2). Jackknife analyses showed that traits for which the ensemble model performance was poorest—such as hemicel-

Table 2. Summary statistics of partial least-squares regression model validation based on full (400–2400 nm) intact- and ground-leaf spectra.

		Intact			Ground				
Litter trait	Range	No. comps	R^2	RMSE	%RMSE	No. comps	R^2	RMSE	%RMSE
C _{mass} (%)	40.9-61.4	12	0.764	1.82	14.0	12	0.689	2.11	16.3
N _{mass} (%)	0.24 - 2.57	15	0.919	0.136	8.58	19	0.946	0.111	7.00
$LMA (g m^{-1})$	39.5-282	11	0.941	15.3	7.49	13	0.842	25.5	12.5
Solubles (%)	27.6-71.4	10	0.794	4.43	14.0	11	0.808	4.33	13.7
Hemicellulose (%)	5.72-26.0	8	0.543	2.79	18.5	8	0.491	2.94	19.5
Recalcitrant carbon (%)	20.7-58.7	11	0.881	2.96	10.0	13	0.887	3.03	10.2
$C_{area} (g m^{-1})$	16.2-172	10	0.940	9.20	8.02				
$N_{area} (g m^{-1})$	0.272-2.43	12	0.766	0.188	13.2				

Note: The range column shows the complete trait range across the full dataset. %root mean squared error (RMSE) is calculated as RMSE divided by the 2.5% trimmed range of data within the validation data set. LMA, leaf mass per area.

Fig. 1. Distributions of spectral reflectance and its coefficient of variation (CV) among intact (left) and ground (right) leaf litter samples. The black line represents the median reflectance at each wavelength, flanked by the 25–75 percentile region (dark blue), and the 2.5–97.5 percentile region (light blue). The solid red line shows the coefficient of variation among spectra at each wavelength.



lulose, C_{mass} , and N_{area} —also had the greatest variability in model performance (Figs. S1 and S2).

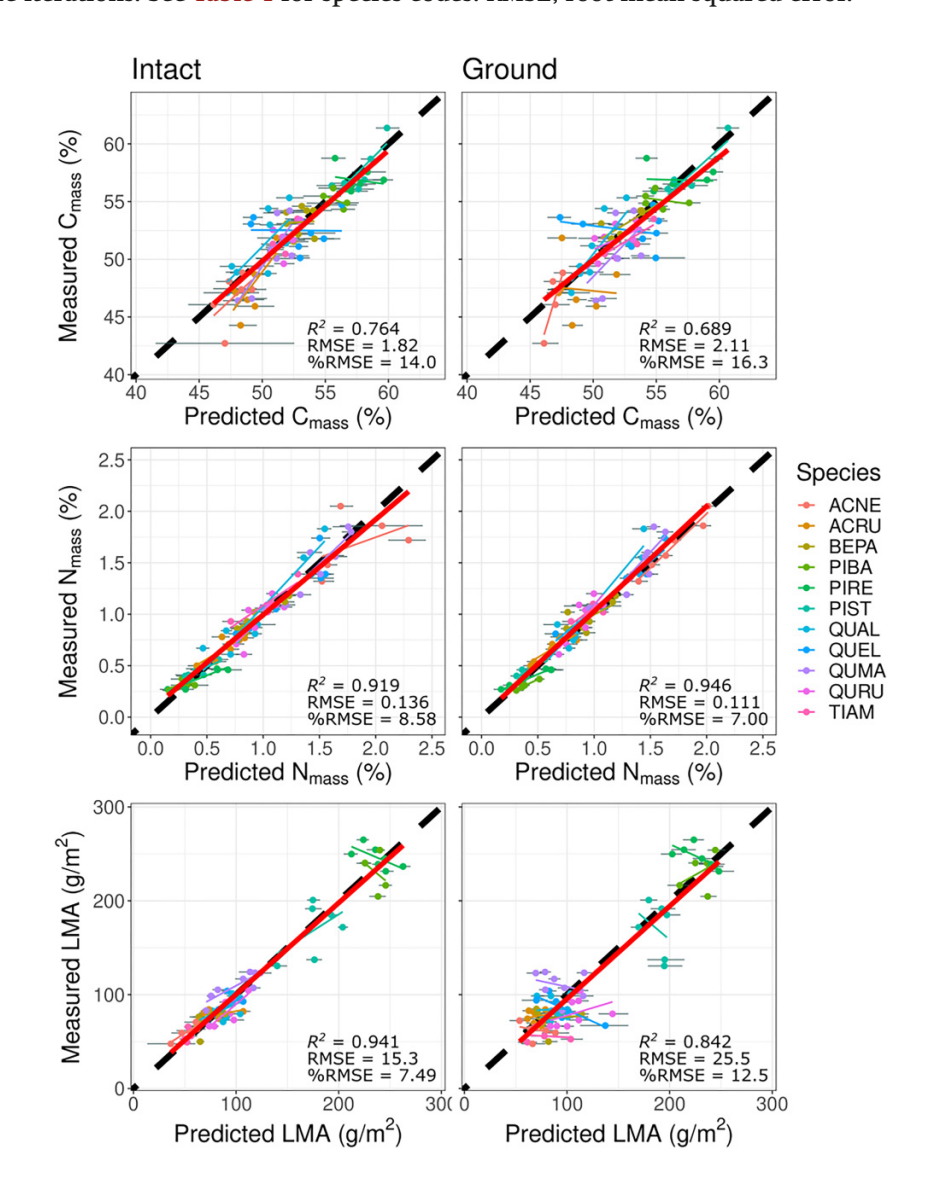
For every trait prediction model trained on the full spectrum, the VIP metric also showed a global maximum around 677 nm (intact) or 672 nm (ground; Fig. 5), next to one of the aforementioned chlorophyll absorption peaks. This pattern suggests that the amount of chlorophyll remaining at abscission may be closely related to many traits. More generally, the visible range was most important for predicting all traits, and the NIR range was also important for LMA. There were further local optima in the SWIR around 1430-1450 nm (for intact leaves), 1910-1950 nm, and 2130-2220 nm. In fresh tissue, variation in reflectance around 1910-1950 nm is often interpreted as a measure of absorption by water, but the trace amounts of water remaining in our dried samples likely have no direct biological relevance. In general, reflectance in the visible range and parts of the SWIR range seemed most informative for predicting nutrients and carbon fractions in litter.

Our VIS/NIR models for intact leaves had considerably worse performance than our full-range models for every trait, particularly N_{mass} , N_{area} , and solubles. By contrast, our SWIR models had very similar performance to the full-range models (Table S2). Both sets of restricted-range models had a similar rank-ordering of model performance across traits to each

other and the full models. Moreover, the VIP metric for these models revealed that the regions that were most important for these predictions were mainly the same bands in their respective regions that were important for the full-range models; however, for the VIS/NIR models, very low wavelengths close to 400 nm also had high importance (Figs. S3–4).

The fact that the CV of intact spectra had maxima at 440-490 and 670-675 nm, and that VIP for many traits had global maxima at 670-680 nm, led us to consider the role of chlorophyll degradation in explaining our ability to predict traits. Both maxima of the CV lie near (but not in the center of) absorption peaks of chlorophylls, and reflectance around 670 nm is particularly sensitive to variation in chlorophyll at low levels, such as during late senescence (Merzlyak et al. 1999). We used two indices, the PSRI and CI_{RE} , to test whether the pigment status of the intact and ground leaves remained informative about other leaf traits. Within species, lower PSRI and higher CI_{RE} were associated with greater N_{mass} , and higher CIRE was also associated with more recalcitrant carbon; these trends were consistent across intact- and groundleaf spectra (Figs. S5-6). For each of these comparisons, the ANCOVAs confirmed the main effect of the pigment index (p < 0.001 in all cases) and of species (p < 0.001 in all cases), as well as an interaction (p < 0.05 in all cases). Although inter-

Fig. 2. Validation results for predictions of solubles, hemicellulose, and recalcitrant carbon from intact-leaf litter spectra (left) and ground-leaf litter spectra (right). In each panel, a thick red line represents the ordinary least squares (OLS) regression fit across the full dataset, while thin colored lines represent each of the 11 species. The thick black dashed line is the 1:1 line. The error bars for each data point are 95% intervals calculated from the distribution of predictions based on the model coefficients from the 200 jackknife iterations. See **Table 1** for species codes. RMSE, root mean squared error.



actions can make it hard to interpret main effects, the plots make it clear that slopes generally had consistent directions across species (Figs. S5–6). In some cases, however, trends across the full dataset diverged from species-specific trends. For example, while intact-leaf CI_{RE} was positively correlated with recalcitrant carbon within species, it was weakly negatively correlated across species (t(314) = -4.34; $R^2 = 0.053$; p < 0.001).

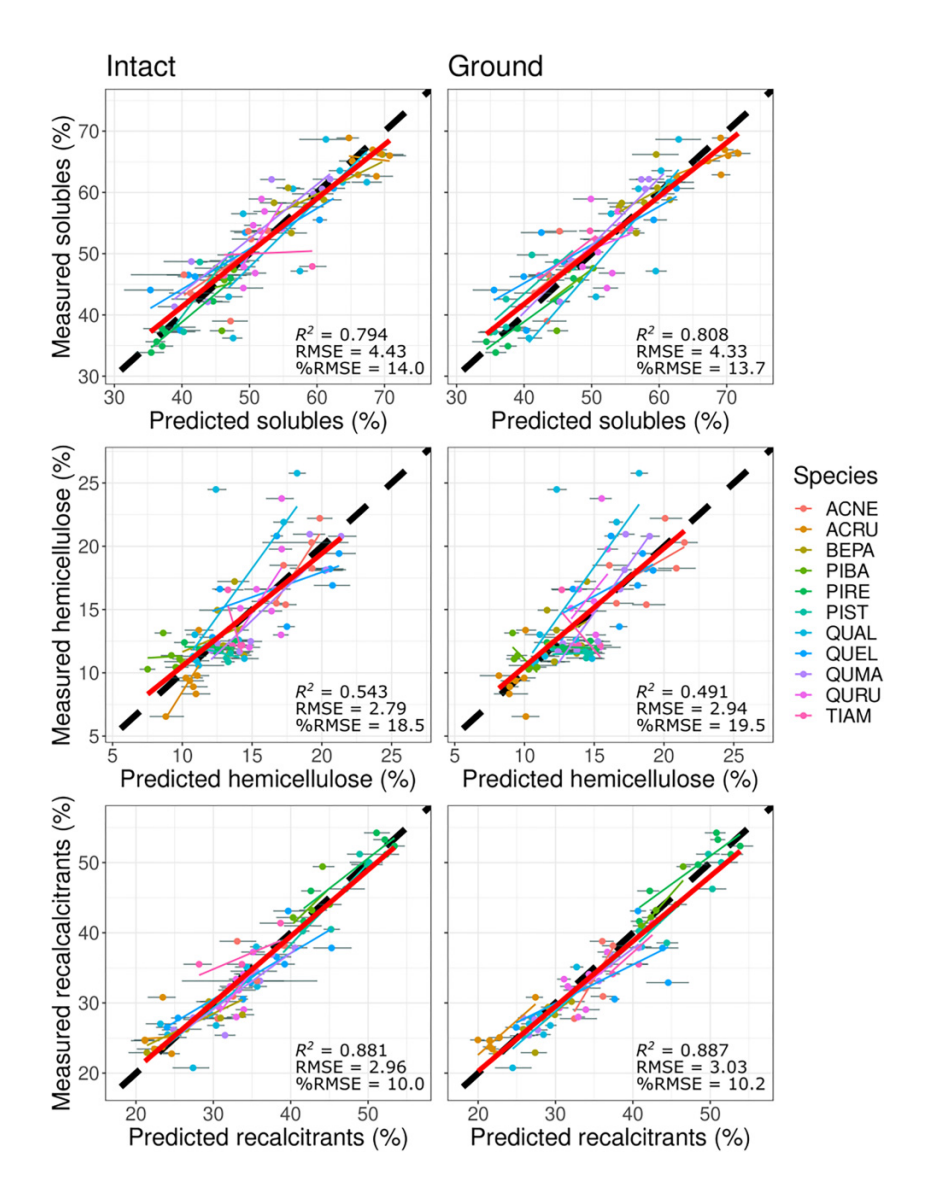
Discussion

We show that PLSR models trained on reflectance spectra can accurately predict several leaf litter traits related to nutrient cycling across temperate broadleaf and needleleaf tree species. For each trait, a single model captures the variation among and within our 11 species. The models' predictions capture well-known ecological differences among functional groups—for example, that needleleaf species have more recalcitrant carbon and lower N_{mass} than broadleaf species. Importantly, intact-leaf models are about as accurate as groundleaf models for most traits, which suggests that multiple traits can be estimated from a single measurement that takes only seconds.

Model performance and interpretation

The hierarchy of which traits can be predicted best mirrors results from non-senesced leaves, including fresh ones (Asner et al. 2011; Nunes et al. 2017; Kothari et al. 2023a). LMA can be predicted very well from intact-leaf spectra in particular, which has been shown in both fresh leaves (Serbin et al. 2019) and in pressed, dried leaves (Costa et al. 2018; Kothari et al. 2023b). Predictions of LMA from ground leaves

Fig. 3. Validation results for predictions of C_{mass}, N_{mass}, and leaf mass per area (LMA) from intact-leaf litter spectra (left) and ground-leaf litter spectra (right). Regression lines and error bars are as in Fig. 2. See Table 1 for species codes. RMSE, root mean squared error.



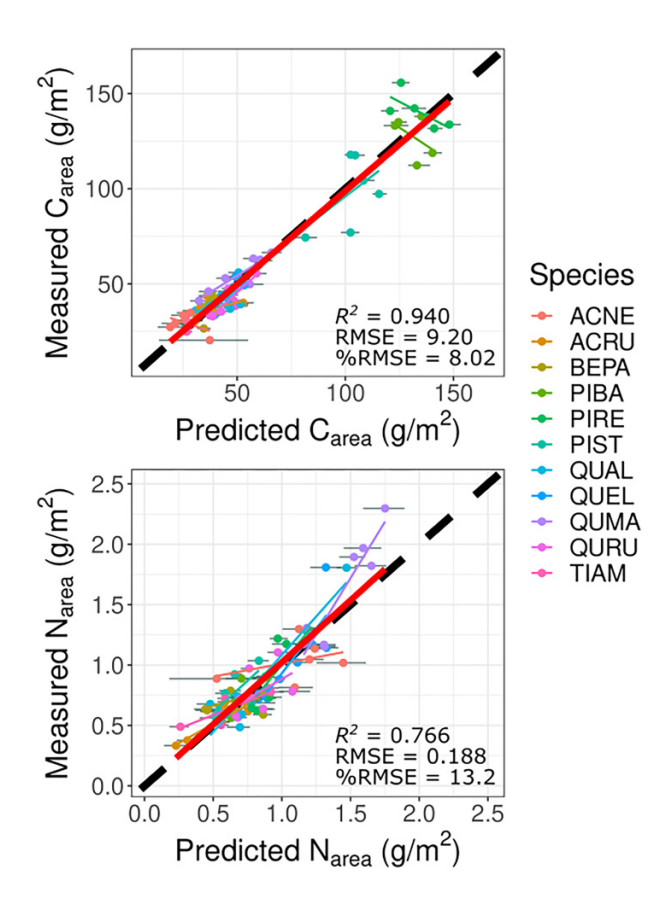
are worse, but still quite good (Serbin et al. 2014). N_{mass} can also be predicted nearly perfectly from intact- and ground-leaf spectra (Richardson and Reeves 2005; Serbin et al. 2014). Recalcitrant carbon, solubles, and C_{mass} all can be predicted with $R^2 > 0.65$, while the smallest carbon fraction (hemicellulose) shows the worst performance (Kothari et al. 2023b). For chemical traits, intact- and ground-leaf models had only small and idiosyncratic differences in performance.

Our comparisons of variation among replicate spectral measurements within samples imply that grinding homogenizes the variation in the leaf and allows more consistent measurements. This consistency may owe to several factors. Veins and other features cause intact leaves to vary in their chemical makeup across the laminar area, which may be hard to capture representatively. Likewise, if chemical traits change with depth through the laminar cross-section, the optical features of deeper layers may be obscured in part by shallower layers. The geometries of uneven needle mats

and curled-up leaves may also reduce consistency by increasing variation in anisotropic surface reflectance (Petibon et al. 2021). Nevertheless, there was no strong, consistent indication that ground-leaf spectra are necessarily better than intact-leaf spectra for predicting chemical traits. This result deviates from the few previous comparisons of intact- and ground-leaf spectra (Serbin et al. 2014; Couture et al. 2016; Kothari et al. 2023b). It is unclear why the theoretical considerations in favor of ground-leaf spectra do not amount to much in practice here; we speculate that information about structure might, depending on the context, either confound or indirectly aid the prediction of chemical traits.

In contrast to chemical traits, LMA was clearly better predicted from intact-leaf spectra. Given that grinding destroys the leaf structure, it may be perplexing that ground-leaf spectra predict structural traits like LMA at all (Serbin et al. 2014; Kothari et al. 2023b). The relationship between ground-leaf spectra and LMA is likely indirect—mediated through corre-

Fig. 4. Validation results for predictions of C_{area} and N_{area} from intact-leaf litter spectra. Regression lines and error bars are as in Fig. 2. See Table 1 for species codes. RMSE, root mean squared error.



lations between LMA and chemical traits that retain clear optical signatures in ground tissue (Nunes et al. 2017). When a model is dependent on this kind of mediation by trait correlations, it may be risky to transfer it to novel settings where the structure of trait correlations may not be the same (Kothari and Schweiger 2022). For example, since trait relationships among species often differ in strength and slope from those within species (Anderegg et al. 2018), a model trained across many species may not accurately capture intraspecific variation (Kothari and Schweiger 2022). Indeed, we found that ground-leaf spectra do a poor job of predicting intraspecific variation in LMA (Fig. 2). Likewise, the relationship between the chlorophyll index CI_{RE} and recalcitrant carbon switches direction between intra- and interspecific scales (Fig. S6).

Changing the basis of nitrogen and carbon from mass to area also changes the accuracy of estimates. While N_{mass} is predicted more accurately than N_{area} , C_{mass} is predicted less accurately than C_{area} . Across samples, N_{mass} correlates negatively and C_{mass} correlates positively with LMA, driven in large part by the split between broadleaf (low LMA) and needleleaf (high LMA) species. As a result, multiplying by LMA to convert N and C to an area basis flattens interspecific variation in N, but enhances it in C. For example, the percentage of variation explained by species identity alone

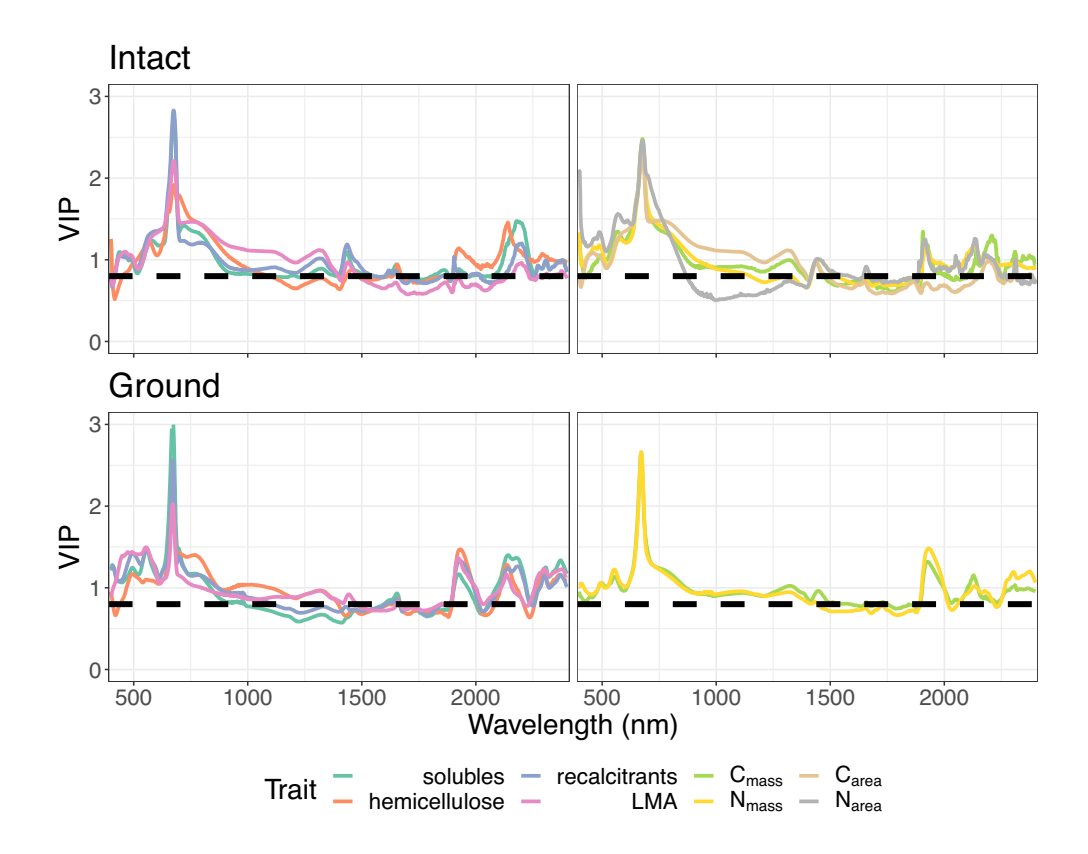
increases for carbon (R^2 from 0.721 for C_{mass} to 0.945 for C_{area}), but decreases for nitrogen (R^2 from 0.786 for N_{mass} to 0.460 N_{area}). Absorption features that differentiate species or functional groups can aid estimates of C_{area} much more than N_{area} , whether or not they are causally related to those traits. Area- and mass-based traits often have different uses: there is a strong justification for using area-based nutrients for studying resorption (van Heerwaarden et al. 2003), while mass-based traits are more often used for explaining decomposition (Cornwell et al. 2008). The basis of estimation should be chosen based on these factors rather than the apparent accuracy of the models.

Visible-range wavelengths where chlorophyll and other pigments absorb had high importance in our main set of fullrange models. However, removing these wavelengths ("SWIR models") did not decrease performance while removing the SWIR range ("VIS/NIR models") did. This finding is in accordance with results from fresh leaves, which often show that the SWIR range has particular importance for accurately predicting many traits (Dechant et al. 2017; Chen et al. 2022). It seems that pigments are neither essential for predictions of litter chemistry, nor do they confound them. Although the bands where they absorb are assigned high importance (Fig. 5) and are correlated with leaf traits within species (Figs. S5–6), much of that information may be redundant with the SWIR range, where many leaf macromolecules absorb. Indeed, given that relationships between visible-range pigment indices and traits are highly variable among species (Figs. S5-6), information from elsewhere in the spectrum may be needed to compensate for these differences. The SWIR models may also transfer better when sample preparation and storage practices are inconsistent, since wavelengths below 1300 nm may be more influenced by pigment degradation (Kothari et al. 2023b).

Advancing spectroscopic estimation of litter traits

Compared to conventional measurements, spectroscopic estimates of plant functional traits are easy and fast to generate and can be non-destructive. Spectrometers are costly, but measuring each spectrum is (on the margin) nearly free. Once samples have been collected and organized, measuring replicate spectra of each intact sample takes under a minute. In contrast, both ground-leaf spectra and conventional measurements require grinding leaves, which is laborious and destructive. Using our protocol, we could measure replicate spectra of a ground sample (including sample tray preparation and cleanup) in 4-7 min, not including grinding time. In contrast, we found that doing both elemental and carbon fraction analysis takes about 25 min of operator time per sample, also not including grinding time. The time saved through spectroscopic trait estimation grows as the number of traits of interest increases. While our models show varying amounts of error, which are generally larger (but not always much larger) than conventional measurements (Serbin et al. 2014), they may aid in studying systems like ours where the variation among species is also considerable. Since the measurements are so rapid, it

Fig. 5. The variable importance of prediction (VIP) metric in intact (top) and ground (bottom) models. The dashed black line represents a threshold of 0.8 suggested as a rough heuristic of importance by **Burnett et al.** (2021).



may also be possible to reduce error by taking more replicate measurements.

Many studies that leverage spectroscopy to address ecological questions use models tailored to the particular species and tissues under study (e.g., McTiernan et al. 2003; Hobbie 2005; Fortunel et al. 2009). While this practice allows researchers more confidence in their trait estimates, it requires them to spend time and money doing the manual trait measurements needed for calibration, which they must repeat for any new study system they adopt. Spectroscopic trait estimation is unlikely to serve as a broad substitute for standard measurements unless we can create models that are demonstrably accurate across a wide range of species and conditions.

The good validation performance of our models does not guarantee accurate trait estimates from any set of litter samples. While our samples vary widely in their traits and optical properties, they all come from temperate trees and are clearly not representative of Earth's plant diversity. When using a model to predict traits for samples with properties beyond those represented in the training data, there is a risk that the results may be biased and misleading (Kothari et al. 2023a). In addition, in instances when models simply "learn" to exploit any features that happen to correspond with a trait among species within a given dataset—without respect to their causal relationship with that trait—they may become overfit and transfer poorly to new settings (Kothari and Schweiger 2022). This case is closely linked to the more

general problem in machine learning of distinguishing spurious and invariant correlations (Arjovsky et al. 2020). As the volume of available spectral data increases, taking care to assess out-of-sample generalization and borrowing tools from machine learning could help us train better spectral models and make more realistic judgments about their performance (Kattenborn et al. 2022; Cherif et al. 2023).

Recent studies have attempted to tackle the challenge of building broad, global trait-spectra models. For example, Serbin et al. (2019) show that a single model can accurately predict the LMA of fresh, non-senesced leaves across 11 sites from the tropics to the Arctic. Although some research has demonstrated trait prediction across stages of senescence or decomposition within single species (Gillon et al. 1999a; Sartori et al. 2022), it remains to be tested whether any single model could achieve this goal across many species. The predictive success of global models for non-senesced leaves may rely on constrained patterns of trait covariation—for example, along continua from sun to shade leaves or conservative to acquisitive leaves (Osnas et al. 2018)—which may cause the relationship between traits and optical features to be relatively invariant (Nunes et al. 2017; Kothari and Schweiger 2022). However, the dramatic shifts in leaf chemistry and cellular structure during senescence (Keskitalo et al. 2005) including pigment degradation and nutrient resorptioncould conceivably weaken the relationships among traits, or between traits and their optical features. If so, it could be hard to build a global model for senesced leaves (or for all

leaves, senesced and not) that achieves the predictive success of global models for fresh green leaves.

Some evidence suggests that litter traits do in fact predictably covary with each other, and with non-senesced leaf traits (Freschet et al. 2010, 2012; Jackson et al. 2013). However, while most fresh green leaves look alike, each species' leaves may have a distinct optical signature of senescence. For example, some of our species (*Acer rubrum*, *Quercus alba*, *Quercus ellipsoidalis*, and *Quercus rubra*) tend to produce reddish anthocyanins, but the rest do not. The breakdown of certain metabolites during senescence also creates a complex mixture of brown pigments (Fourty et al. 1996), which are poorly described and could vary from species to species. Such variation could make the relationship between traits and optical features more contingent for senescent foliage.

Even setting aside these concerns, model generality may also be complicated by factors like storage conditions, sample preparation (e.g., grind size), and instruments, which may affect the spectrum in subtle but important ways (Foley et al. 1998; Petibon et al. 2021). Overcoming these challenges may require investing in protocol development, or in trying algorithms that are more flexible than PLSR in "learning" the complex signatures of biological variation in heterogeneous datasets. In the meantime, it may be prudent for researchers who use existing spectral models in new systems to continue to take some conventional trait measurements to validate model performance.

Finally, we note that plants produce and shed many kinds of tissue besides leaves, and these other litter sources also contribute to nutrient cycling through resorption and decomposition (Lü et al. 2012). Reflectance spectroscopy may help measure nutrient-related traits in other tissues. For example, fine root senescence is an important but little-understood part of nutrient cycling; fine roots may contribute nearly half of annual litter inputs in forests (Freschet et al. 2013) and vary considerably in resorption efficiency (Freschet et al. 2010). Elle et al. (2019) showed that PLSR models built using NIR reflectance spectroscopy can predict fine root lignin, which generally increases recalcitrance (See et al. 2019). Continuing to develop models for other plant tissues could make it easier to study how plants alter nutrient cycling in a holistic way.

Likewise, nutrient cycling is influenced by traits beyond those we considered. For example, although we could not separate cellulose and lignin for methodological reasons, they may have distinct influences on decomposition, and it would be ideal to build separate models for them (Talbot and Treseder 2012). In addition, nutrients other than nitrogen often limit or co-limit decomposition (Cornwell et al. 2008; Keiluweit et al. 2015), and phosphorus resorption may be an important part of nutrient economies when phosphorus limits growth (Hayes et al. 2014). However, estimates of some micronutrients from reflectance spectra may be unreliable (Nunes et al. 2017; Kothari et al. 2023a), and other methods may prove more useful (e.g., X-ray fluorescence spectroscopy; van der Ent et al. 2018).

Ultimately, whether accurate global models can be built to predict litter traits from spectra is an empirical question that can only be settled by amassing a wide variety of data from across ecosystems and growth forms. We take an initial step toward this long-term goal by showing that reflectance spectroscopy can provide accurate litter trait estimates across many temperate tree species that vary widely in their litter traits. This line of research shows great promise in relieving some of the major limitations toward understanding plant functional ecology in an ecosystem context.

Acknowledgements

The University of Minnesota, including Cedar Creek, is located on the traditional and contemporary Dakota and Ojibwe land. Many members of the Cavender-Bares Lab and the UMN Physiological Ecology Discussion Group contributed to discussions that improved this paper. We give particular thanks to Laura Williams, Artur Stefanski, Sam Reed, and Habacuc Flores-Moreno for useful discussions and help in data collection, as well as Rebecca Montgomery for contributions to the FAB1 experiment. The research was supported by an Alexander and Lydia Anderson Grant from University of Minnesota and by the National Science Foundation's funding of Cedar Creek LTER under DEB #1234162. Spectral measurements were conducted as part of an NSF/NASA Dimensions of Biodiversity project (DEB #1342778) and the NSF AS-CEND Biology Integration Institute (DBI #2021898). SK was supported by an NSF Graduate Research Fellowship (Grant No. 00039202) and a UMN Doctoral Dissertation Fellowship.

Article information

History dates

Received: 28 November 2023 Accepted: 10 April 2024

Accepted manuscript online: 24 April 2024 Version of record online: 14 August 2024

Copyright

© 2024 The Author(s). Permission for reuse (free in most cases) can be obtained from copyright.com.

Data availability

Spectral and trait data and coefficients of PLSR models can be found on EcoSIS (Kothari et al. 2024a, 2024b). Analysis code is available at https://github.com/ShanKothari/senesced-traitmodels; a version is archived on Zenodo (Kothari 2024).

Author information

Author ORCIDs

Shan Kothari https://orcid.org/0000-0001-9445-5548

Author notes

Present address for Shan Kothari is Centre d'étude de la forêt, Université du Québec à Montréal, Montréal, QC H2X 3Y7, Canada.

Author contributions

Conceptualization: SK, SEH, JC

Data curation: SK Formal analysis: SK Funding acquisition: SEH, JC

Investigation: SK Methodology: SK

Project administration: SK, JC

Software: SK Supervision: JC Visualization: SK

Writing - original draft: SK

Writing - review & editing: SK, SEH, JC

Competing interests

The authors have no competing interests to declare.

Supplementary material

References

- Anderegg, L.D.L., Berner, L.T., Badgley, G., Sethi, M.L., Law, B.E., and HilleRisLambers, J. 2018. Within-species patterns challenge our understanding of the leaf economics spectrum. Ecology Letters 21(5): 734–744. doi:10.1111/ele.12945.
- Arjovsky, M., Bottou, L., Gulrajani, I., and Lopez-Paz, D. 2020. Invariant risk minimization (arXiv:1907.02893). arXiv. doi:10.48550/arXiv. 1907.02893.
- Asner, G.P., Martin, R.E., Knapp, D.E., Tupayachi, R., Anderson, C., Carranza, L., et al. 2011. Spectroscopy of canopy chemicals in humid tropical forests. Remote Sens. Environ. 115(12): 3587–3598. doi:10. 1016/j.rse.2011.08.020.
- Berg, B. 2014. Decomposition patterns for foliar litter—a theory for influencing factors. Soil Biol. Biochem. **78**: 222–232. doi:10.1016/j.soilbio. 2014.08.005.
- Blackburn, G.A. 1998. Quantifying chlorophylls and caroteniods at leaf and canopy scales: an evaluation of some hyperspectral approaches. Remote Sens. Environ. 66(3): 273–285. doi:10.1016/S0034-4257(98) 00059-5.
- Bourget, M.Y., Fanin, N., Fromin, N., Hättenschwiler, S., Roumet, C., Shihan, A., et al. 2023. Plant litter chemistry drives long-lasting changes in the catabolic capacities of soil microbial communities. Funct. Ecol. 37(7): 2014–2028. doi:10.1111/1365-2435.14379.
- Burnett, A.C., Anderson, J., Davidson, K.J., Ely, K.S., Lamour, J., Li, Q., et al. 2021. A best-practice guide to predicting plant traits from leaf-level hyperspectral data using partial least squares regression. J. Exp. Bot. 72(18): 6175–6189. doi:10.1093/jxb/erab295. PMID: 34131723.
- Cavender-Bares, J., Schweiger, A.K., Gamon, J.A., Gholizadeh, H., Helzer, K., Lapadat, C., et al. 2022. Remotely detected aboveground plant function predicts belowground processes in two prairie diversity experiments. Ecol. Monogr. 92(1): e01488. doi:10.1002/ecm.1488. PMID: 35864994.
- Chapin, F.S., III, and Moilanen, L. 1991. Nutritional controls over nitrogen and phosphorus resorption from Alaskan birch leaves. Ecology, **72**(2): 709–715. doi:10.2307/2937210.
- Chavana-Bryant, C., Malhi, Y., Wu, J., Asner, G.P., Anastasiou, A., Enquist, B.J., et al. 2017. Leaf aging of Amazonian canopy trees as revealed by spectral and physiochemical measurements. New Phytol. **214**(3): 1049–1063. doi:10.1111/nph.13853. PMID: 26877108.
- Chen, L., Zhang, Y., Nunes, M.H., Stoddart, J., Khoury, S., Chan, A.H.Y., and Coomes, D.A. 2022. Predicting leaf traits of temperate broadleaf deciduous trees from hyperspectral reflectance: Can a general model be applied across a growing season? Remote Sens. Environ. **269**: 112767. doi:10.1016/j.rse.2021.112767.
- Cherif, E., Feilhauer, H., Berger, K., Dao, P.D., Ewald, M., Hank, T.B., et al. 2023. From spectra to plant functional traits: transferable multi-trait models from heterogeneous and sparse data. Remote Sens. Environ. 292: 113580. doi:10.1016/j.rse.2023.113580.

- Cornelissen, J.H.C., Pérez-Harguindeguy, N., Díaz, S., Grime, J.P., Marzano, B., Cabido, M., et al. 1999. Leaf structure and defence control litter decomposition rate across species and life forms in regional floras on two continents. New Phytol. 143(1): 191–200. doi:10.1046/j. 1469-8137.1999.00430.x.
- Cornwell, W.K., Cornelissen, J.H.C., Amatangelo, K., Dorrepaal, E., Eviner, V.T., Godoy, O., et al. 2008. Plant species traits are the predominant control on litter decomposition rates within biomes worldwide. Ecol. Lett. 11(10): 1065–1071. doi:10.1111/j.1461-0248.2008.01219.x. PMID: 18627410.
- Costa, F.R.C., Lang, C., Almeida, D.R.A., Castilho, C.V., and Poorter, L. 2018. Near-infrared spectrometry allows fast and extensive predictions of functional traits from dry leaves and branches. Ecol. Appl. **28**(5): 1157–1167. doi:10.1002/eap.1728. PMID: 29768699.
- Cotrozzi, L., Couture, J.J., Cavender-Bares, J., Kingdon, C.C., Fallon, B., Pilz, G., et al. 2017. Using foliar spectral properties to assess the effects of drought on plant water potential. Tree Physiol. **37**(11): 1582–1591. doi:10.1093/treephys/tpx106. PMID: 29036552.
- Coûteaux, M.-M., Sarmiento, L., Hervé, D., and Acevedo, D. 2005. Determination of water-soluble and total extractable polyphenolics in biomass, necromass and decomposing plant material using near-infrared reflectance spectroscopy (NIRS). Soil Biol. Biochem. 37(4): 795–799. doi:10.1016/j.soilbio.2004.08.028.
- Couture, J.J., Singh, A., Rubert-Nason, K.F., Serbin, S.P., Lindroth, R.L., and Townsend, P.A. 2016. Spectroscopic determination of ecologically relevant plant secondary metabolites. Methods Ecol. Evol. **7**(11): 1402–1412. doi:10.1111/2041-210X.12596.
- Curran, P.J. 1989. Remote sensing of foliar chemistry. Remote Sens. Environ. **30**(3): 271–278. doi:10.1016/0034-4257(89)90069-2.
- Dechant, B., Cuntz, M., Vohland, M., Schulz, E., and Doktor, D. 2017. Estimation of photosynthesis traits from leaf reflectance spectra: correlation to nitrogen content as the dominant mechanism. Remote Sens. Environ. 196: 279–292. doi:10.1016/j.rse.2017.05.019.
- Diehl, P., Mazzarino, M.J., Funes, F., Fontenla, S., Gobbi, M., and Ferrari, J. 2003. Nutrient conservation strategies in native Andean-Patagonian forests. J. Veg. Sci. 14(1): 63–70. doi:10.1111/j.1654-1103. 2003.tb02128.x.
- El Zein, R., Bréda, N., Gérant, D., Zeller, B., and Maillard, P. 2011. Nitrogen sources for current-year shoot growth in 50-year-old sessile oak trees: an in situ 15 N labeling approach. Tree Physiol. 31(12): 1390–1400. doi:10.1093/treephys/tpr118. PMID: 22158010.
- Elle, O., Richter, R., Vohland, M., and Weigelt, A. 2019. Fine root lignin content is well predictable with near-infrared spectroscopy. Sci. Rep. **9**(1): 6396. doi:10.1038/s41598-019-42837-z. PMID: 31015553.
- Feilhauer, H., Asner, G.P., Martin, R.E., and Schmidtlein, S. 2010. Brightness-normalized partial least squares regression for hyperspectral data. J. Quant. Spectrosc. Radiat. Transfer, 111(12): 1947–1957. doi:10.1016/j.jqsrt.2010.03.007.
- Foley, W.J., McIlwee, A., Lawler, I., Aragones, L., Woolnough, A.P., and Berding, N. 1998. Ecological applications of near infrared reflectance spectroscopy—a tool for rapid, cost-effective prediction of the composition of plant and animal tissues and aspects of animal performance. Oecologia, 116(3): 293–305. doi:10.1007/s004420050591. PMID: 28308060.
- Fortunel, C., Garnier, E., Joffre, R., Kazakou, E., Quested, H., Grigulis, K., et al. 2009. Leaf traits capture the effects of land use changes and climate on litter decomposability of grasslands across Europe. Ecology, 90(3): 598–611. doi:10.1890/08-0418.1.
- Fourty, T., Baret, F., Jacquemoud, S., Schmuck, G., and Verdebout, J. 1996. Leaf optical properties with explicit description of its biochemical composition: direct and inverse problems. Remote Sens. Environ. **56**(2): 104–117. doi:10.1016/0034-4257(95)00234-0.
- Freschet, G.T., Aerts, R., and Cornelissen, J.H.C. 2012. A plant economics spectrum of litter decomposability. Funct. Ecol. **26**(1): 56–65. doi:10. 1111/j.1365-2435.2011.01913.x.
- Freschet, G.T., Cornelissen, J.H.C., Logtestijn, R.S.P., and Aerts, R. 2010. Substantial nutrient resorption from leaves, stems and roots in a subarctic flora: What is the link with other resource economics traits? New Phytol. **186**(4): 879–889. doi:10.1111/j.1469-8137.2010.03228.x. PMID: 20345640.
- Freschet, G.T., Cornwell, W.K., Wardle, D.A., Elumeeva, T.G., Liu, W., Jackson, B.G., et al. 2013. Linking litter decomposition of above-

- and below-ground organs to plant-soil feedbacks worldwide. J. Ecol. **101**(4): 943–952. doi:10.1111/1365-2745.12092.
- Gill, A.L., Schilling, J., and Hobbie, S.E. 2021. Experimental nitrogen fertilisation globally accelerates, then slows decomposition of leaf litter. Ecol. Lett. **24**(4): 802–811. doi:10.1111/ele.13700. PMID: 33583093.
- Gillon, D., Houssard, C., and Joffre, R. 1999a. Using near-infrared reflectance spectroscopy to predict carbon, nitrogen and phosphorus content in heterogeneous plant material. Oecologia, **118**(2): 173–182. doi:10.1007/s004420050716. PMID: 28307692.
- Gillon, D., Joffre, R., and Ibrahima, A. 1999b. Can litter decomposability be predicted by near infrared reflectance spectroscopy? Ecology, **80**(1): 175–186. doi:10.1890/0012-9658(1999)080%5b0175: CLDBPB%5d2.0.CO;2.
- Gitelson, A.A., Chivkunova, O.B., and Merzlyak, M.N. 2009. Nondestructive estimation of anthocyanins and chlorophylls in anthocyanic leaves. Am. J. Bot. **96**(10): 1861–1868. doi:10.3732/ajb.0800395. PMID: 21622307.
- Grossman, J.J., Cavender-Bares, J., and Hobbie, S.E. 2020. Functional diversity of leaf litter mixtures slows decomposition of labile but not recalcitrant carbon over two years. Ecol. Monogr. **90**(3): e01407. doi:10.1002/ecm.1407.
- Grossman, J.J., Cavender-Bares, J., Hobbie, S.E., Reich, P.B., and Montgomery, R.A. 2017. Species richness and traits predict overyielding in stem growth in an early-successional tree diversity experiment. Ecology, 98(10): 2601–2614. doi:10.1002/ecy.1958. PMID: 28727905.
- Hayes, P., Turner, B.L., Lambers, H., and Laliberté, E. 2014. Foliar nutrient concentrations and resorption efficiency in plants of contrasting nutrient-acquisition strategies along a 2-million-year dune chronosequence. J. Ecol. 102(2): 396–410. doi:10.1111/1365-2745. 12196.
- Hobbie, S.E. 2005. Contrasting effects of substrate and fertilizer nitrogen on the early stages of litter decomposition. Ecosystems, **8**(6): 644–656. doi:10.1007/s10021-003-0110-7.
- Hobbie, S.E. 2015. Plant species effects on nutrient cycling: revisiting litter feedbacks. Trends Ecol. Evol. **30**(6): 357–363.
- Jackson, B.G., Peltzer, D.A., and Wardle, D.A. 2013. Are functional traits and litter decomposability coordinated across leaves, twigs and wood? A test using temperate rainforest tree species. Oikos, 122(8): 1131–1142. doi:10.1111/j.1600-0706.2012.00056.x.
- Joffre, R., Gillon, D., Dardenne, P., Agneessens, R., and Biston, R. 1992. The use of near-infrared reflectance spectroscopy in litter decomposition studies. Ann. Sci. For. 49(5): 481–488. doi:10.1051/forest: 19920504.
- Kattenborn, T., Schiefer, F., Frey, J., Feilhauer, H., Mahecha, M.D., and Dormann, C.F. 2022. Spatially autocorrelated training and validation samples inflate performance assessment of convolutional neural networks. ISPRS Open J. Photogramm. Remote Sens. 5: 100018. doi:10.1016/j.ophoto.2022.100018.
- Keiluweit, M., Nico, P., Harmon, M.E., Mao, J., Pett-Ridge, J., and Kleber, M. 2015. Long-term litter decomposition controlled by manganese redox cycling. Proc. Natl. Acad. Sci. USA, 112(38): E5253–E5260. doi:10.1073/ pnas.1508945112.
- Keskitalo, J., Bergquist, G., Gardeström, P., and Jansson, S. 2005. A cellular timetable of autumn senescence. Plant Physiol. **139**(4): 1635–1648. doi:10.1104/pp.105.066845.
- Kobe, R.K., Lepczyk, C.A., and Iyer, M. 2005. Resorption efficiency decreases with increasing green leaf nutrients in a global data set. Ecology, 86(10): 2780–2792. doi:10.1890/04-1830.
- Kothari, S. 2024. ShanKothari/senesced-trait-models: fix bug release for MPLS samples (0.0.3). Zenodo. doi:10.5281/zenodo.10969552.
- Kothari, S., and Schweiger, A.K. 2022. Plant spectra as integrative measures of plant phenotypes. J. Ecol. **110**(11): 2536–2554. doi:10.1111/1365-2745.13972.
- Kothari, S., Beauchamp-Rioux, R., Blanchard, F., Crofts, A.L., Girard, A., Guilbeault-Mayers, X., et al. 2023a. Predicting leaf traits across functional groups using reflectance spectroscopy. New Phytol. 238(2): 549–566. doi:10.1111/nph.18713.
- Kothari, S., Beauchamp-Rioux, R., Laliberté, E., and Cavender-Bares, J. 2023b. Reflectance spectroscopy allows rapid, accurate and nondestructive estimates of functional traits from pressed leaves. Methods Ecol. Evol. 14: 385–401. doi:10.1111/2041-210X.13958.

- Kothari, S., Hobbie, S., and Cavender-Bares, J. 2024a. Intact- and ground-leaf litter spectra from Cedar Creek and Minneapolis [Dataset]. Dryad. doi:10.5061/dryad.hdr7sqvrk.
- Kothari, S., Hobbie, S., and Cavender-Bares, J. 2024b. Models for rapid estimates of leaf litter chemistry using reflectance spectroscopy [Datatset]. Dryad. doi:10.5061/dryad.hdr7sqvrg.
- Kruse, F.A., Lefkoff, A.B., Boardman, J.W., Heidebrecht, K.B., Shapiro, A.T., Barloon, P.J., and Goetz, A.F.H. 1993. The spectral image processing system (SIPS)—interactive visualization and analysis of imaging spectrometer data. Remote Sens. Environ. 44(2): 145–163. doi:10.1016/ 0034-4257(93)90013-N.
- Liu, J., Liu, X., Song, Q., Compson, Z.G., LeRoy, C.J., Luan, F., et al. 2020. Synergistic effects: a common theme in mixed-species litter decomposition. New Phytol. 227(3): 757–765. doi:10.1111/nph.16556.
- Lü, X.-T., Freschet, G.T., Flynn, D.F.B., and Han, X.-G. 2012. Plasticity in leaf and stem nutrient resorption proficiency potentially reinforces plant–soil feedbacks and microscale heterogeneity in a semiarid grassland. J. Ecol. 100(1): 144–150. doi:10.1111/j.1365-2745.2011. 01881.x.
- Madritch, M., Cavender-Bares, J., Hobbie, S.E., and Townsend, P. 2020. Linking foliar traits to belowground processes. *In Remote sensing of plant biodiversity*. *Edited by J. Cavender-Bares*, J. Gamon and P. Townsend. Springer, New York. pp. 173–198.
- McTiernan, K.B., Coûteaux, M.-M., Berg, B., Berg, M.P., Calvo de Anta, R., Gallardo, A., et al. 2003. Changes in chemical composition of Pinus sylvestris needle litter during decomposition along a European coniferous forest climatic transect. Soil Biol. Biochem. 35(6): 801–812. doi:10.1016/S0038-0717(03)00107-X.
- Meireles, J.E., Schweiger, A.K., and Cavender-Bares, J. 2023. spectrolab: Class and methods for spectral data in R. R package v.0.0.18. [WWW document]. Available from https://CRAN.R-project.org/package=spectrolab [accessed September 2023].
- Merzlyak, M.N., Gitelson, A.A., Chivkunova, O.B., and Rakitin, V.Y.U. 1999. Non-destructive optical detection of pigment changes during leaf senescence and fruit ripening. Physiol. Plant. **106**(1): 135–141. doi:10.1034/j.1399-3054.1999.106119.x.
- Mevik, B.-H., Wehrens, R., and Liland, K.H. 2019. PLS: partial least squares and principal component regression. R package v.2.7-1. [WWW document]. Available from https://CRAN.R-project.org/package=pls [accessed September 2023].
- Norris, K.H., Barnes, R.F., Moore, J.E., and Shenk, J.S. 1976. Predicting forage quality by infrared reflectance spectroscopy. J. Anim. Sci. 43(4): 889–897. doi:10.2527/jas1976.434889x.
- Nunes, M.H., Davey, M.P., and Coomes, D.A. 2017. On the challenges of using field spectroscopy to measure the impact of soil type on leaf traits. Biogeosciences, 14(13): 3371–3385. doi:10.5194/bg-14-3371-2017.
- Osnas, J.L.D., Katabuchi, M., Kitajima, K., Wright, S.J., Reich, P.B., Bael, S.A.V., et al. 2018. Divergent drivers of leaf trait variation within species, among species, and among functional groups. Proc. Natl. Acad. Sci. USA, 115(21): 5480–5485. doi:10.1073/pnas.1803989115.
- Parsons, S.A., Lawler, I.R., Congdon, R.A., and Williams, S.E. 2011. Rainforest litter quality and chemical controls on leaf decomposition with near-infrared spectrometry. J. Plant Nutr. Soil Sci. 174(5): 710–720. doi:10.1002/jpln.201100093.
- Perez, T.M., Rodriguez, J., and Heberling, J.M. 2020. Herbarium-based measurements reliably estimate three functional traits. Am. J. Bot. **107**(10): 1457–1464. doi:10.1002/ajb2.1535.
- Petibon, F., Czyż, E.A., Ghielmetti, G., Hueni, A., Kneubühler, M., Schaepman, M.E., and Schuman, M.C. 2021. Uncertainties in measurements of leaf optical properties are small compared to the biological variation within and between individuals of European beech. Remote Sens. Environ. 264: 112601. doi:10.1016/j.rse.2021.112601.
- Petit Bon, M., Böhner, H., Kaino, S., Moe, T., and Bråthen, K.A. 2020. One leaf for all: chemical traits of single leaves measured at the leaf surface using near-infrared reflectance spectroscopy. Methods Ecol. Evol. 11(9): 1061–1071. doi:10.1111/2041-210X.13432.
- Prescott, C.E. 2010. Litter decomposition: What controls it and how can we alter it to sequester more carbon in forest soils? Biogeochemistry, **101**(1): 133–149. doi:10.1007/s10533-010-9439-0.
- R Core Team. 2022. R: a language and environment for statistical computing. R Foundation for Statistical Computing, Vienna, Austria. [WWW document]. Available from https://www.R-project.org/ [accessed 9 March 2020].

- Rea, A.M., Mason, C.M., and Donovan, L.A. 2018. Evolution of nutrient resorption across the herbaceous genus *Helianthus*. Plant Ecol. **219**(8): 887–899. doi:10.1007/s11258-018-0841-3.
- Reeves, J.B. 2009. Does the spectral format matter in diffuse reflection spectroscopy? Appl. Spectrosc. **63**(6): 669–677. doi:10.1366/000370209788559692.
- Richardson, A.D., and Reeves, J.B., III. 2005. Quantitative reflectance spectroscopy as an alternative to traditional wet lab analysis of foliar chemistry: near-infrared and mid-infrared calibrations compared. Can. J. For. Res. 35(5): 1122–1130. doi:10.1139/x05-037.
- Sartori, K., Violle, C., Vile, D., Vasseur, F., de Villemereuil, P., Bresson, J., et al. 2022. Do leaf nitrogen resorption dynamics align with the slow-fast continuum? A test at the intraspecific level. Funct. Ecol. **36**(5): 1315–1328. doi:10.1111/1365-2435.14029.
- Schreeg, L.A., Mack, M.C., and Turner, B.L. 2013. Nutrient-specific solubility patterns of leaf litter across 41 lowland tropical woody species. Ecology, **94**(1): 94–105. doi:10.1890/11-1958.1.
- Schweitzer, J.A., Bailey, J.K., Rehill, B.J., Martinsen, G.D., Hart, S.C., Lindroth, R.L., et al. 2004. Genetically based trait in a dominant tree affects ecosystem processes. Ecol. Lett. **7**(2): 127–134. doi:10.1111/j. 1461-0248.2003.00562.x.
- See, C.R., McCormack, M.L., Hobbie, S.E., Flores-Moreno, H., Silver, W.L., and Kennedy, P.G. 2019. Global patterns in fine root decomposition: climate, chemistry, mycorrhizal association and woodiness. Ecol. Lett. 22(6): 946–953. doi:10.1111/ele.13248.
- Serbin, S.P., Singh, A., McNeil, B.E., Kingdon, C.C., and Townsend, P.A. 2014. Spectroscopic determination of leaf morphological and biochemical traits for northern temperate and boreal tree species. Ecol. Appl. 24(7): 1651–1669. doi:10.1890/13-2110.1.

- Serbin, S.P., Wu, J., Ely, K.S., Kruger, E.L., Townsend, P.A., Meng, R., et al. 2019. From the Arctic to the tropics: multibiome prediction of leaf mass per area using leaf reflectance. New Phytol. **224**(4): 1557–1568. doi:10.1111/nph.16123.
- Talbot, J.M., and Treseder, K.K. 2012. Interactions among lignin, cellulose, and nitrogen drive litter chemistry–decay relationships. Ecology, **93**(2): 345–354. doi:10.1890/11-0843.1.
- van der Ent, A., Przybyłowicz, W.J., de Jonge, M.D., Harris, H.H., Ryan, C.G., Tylko, G., et al. 2018. X-ray elemental mapping techniques for elucidating the ecophysiology of hyperaccumulator plants. New Phytol. **218**(2): 432–452. doi:10.1111/nph.14810.
- van Heerwaarden, L.M., Toet, S., and Aerts, R. 2003. Current measures of nutrient resorption efficiency lead to a substantial underestimation of real resorption efficiency: facts and solutions. Oikos, **101**(3): 664–669. doi:10.1034/j.1600-0706.2003.12351.x.
- Vergutz, L., Manzoni, S., Porporato, A., Novais, R.F., and Jackson, R.B. 2012. Global resorption efficiencies and concentrations of carbon and nutrients in leaves of terrestrial plants. Ecol. Monogr. **82**(2): 205–220. doi:10.1890/11-0416.1.
- Wold, S. 1994. PLS for multivariate linear modeling. In Chemometric methods in molecular design, methods and principles in medicinal chemistry. Edited by H. van de Waterbeemd. Verlag-Chemie, Weinheim, Germany. pp. 195–218.
- Wright, I.J., and Westoby, M. 2003. Nutrient concentration, resorption and lifespan: leaf traits of Australian sclerophyll species. Funct. Ecol. 17(1): 10–19. doi:10.1046/j.1365-2435.2003.00694.x.
- Yuan, Z.Y., and Chen, H.Y.H. 2015. Negative effects of fertilization on plant nutrient resorption. Ecology, **96**(2): 373–380. doi:10.1890/14-0140.1.

Copyright of Canadian Journal of Forest Research is the property of Canadian Science Publishing and its content may not be copied or emailed to multiple sites or posted to a listserv without the copyright holder's express written permission. However, users may print, download, or email articles for individual use.